Electronic Supplementary Material (ESI) for Dalton Transactions.

High-sensitive optical temperature sensing based on upconversion luminescence in $Gd_{9.33}(SiO_4)_6O_2$:Yb^{3+}-Er^{3+}/Ho^{3+} phosphors

Jia Zhang[1,2,*], Fangsheng Qian[1]

[1]Physics department and Jiangsu Key Laboratory of Modern Measurement Technology and Intelligence, Huaiyin Normal University, 111 West Chang Jiang Road, Huai'an 223300, China

[2]Jiangsu Key Laboratory for Chemistry of Low-Dimensional Materials, Huaiyin Normal University, 111 West Chang Jiang Road, Huai'an 223300, China

*Corresponding author.

E-mail address: zhangjianew@126.com

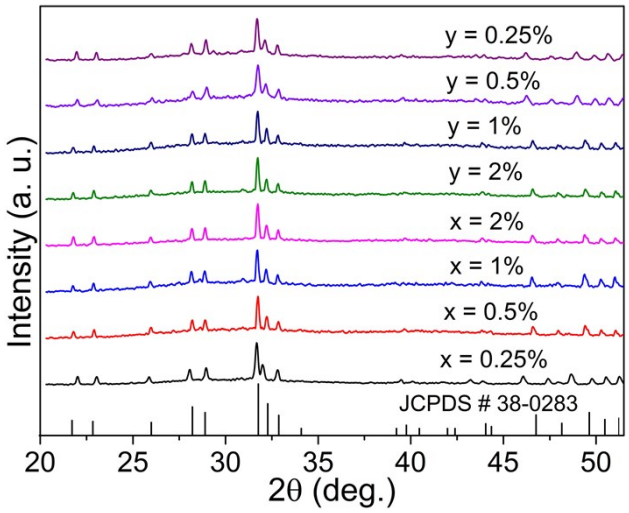

Fig. S1 XRD patterns of GSO:10%Yb^{3+},xEr^{3+} (0.25% ≤ x ≤ 2%) and GSO:10%Yb^{3+},yHo^{3+} (0.25% ≤ y ≤ 2%)

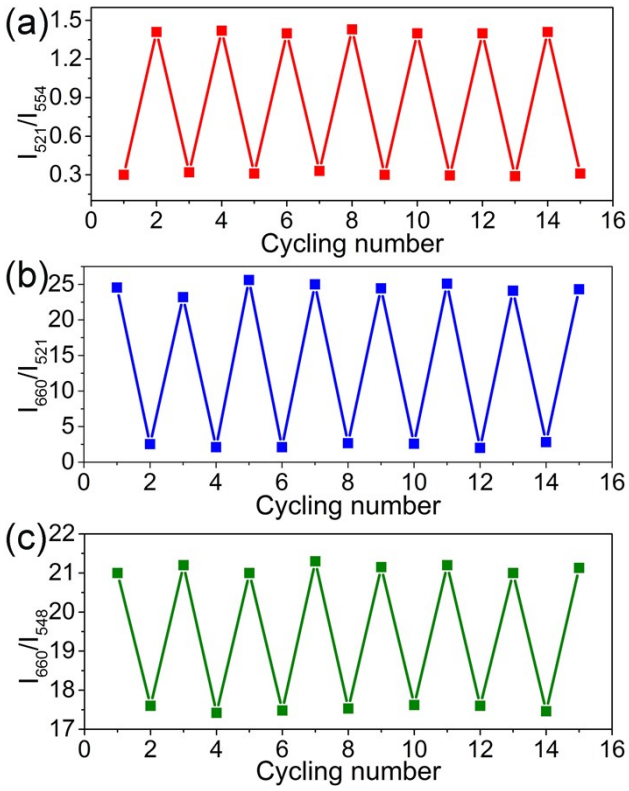

Fig. S2 Temperature-induced switching of (a) I_{521}/I_{554} and (b) I_{660}/I_{521} for GSO:10%Yb^{3+},1%Er^{3+} as well as (c) I_{660}/I_{548} for GSO:10%Yb^{3+},0.25%Ho^{3+}

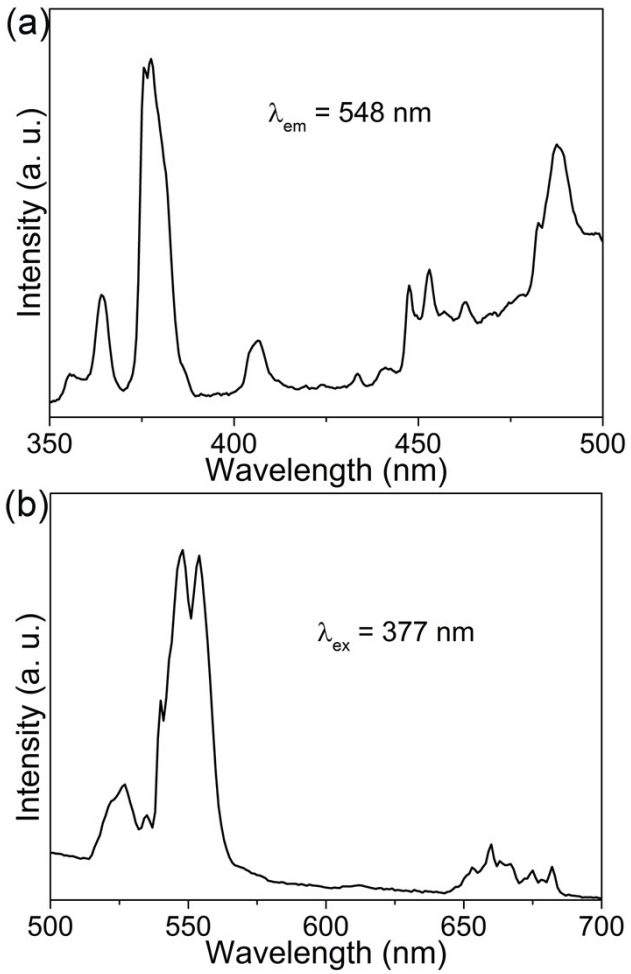

Fig. S3 (a) Excitation and (b) emission spectra of GSO:10%Yb^{3+},1%Er^{3+}

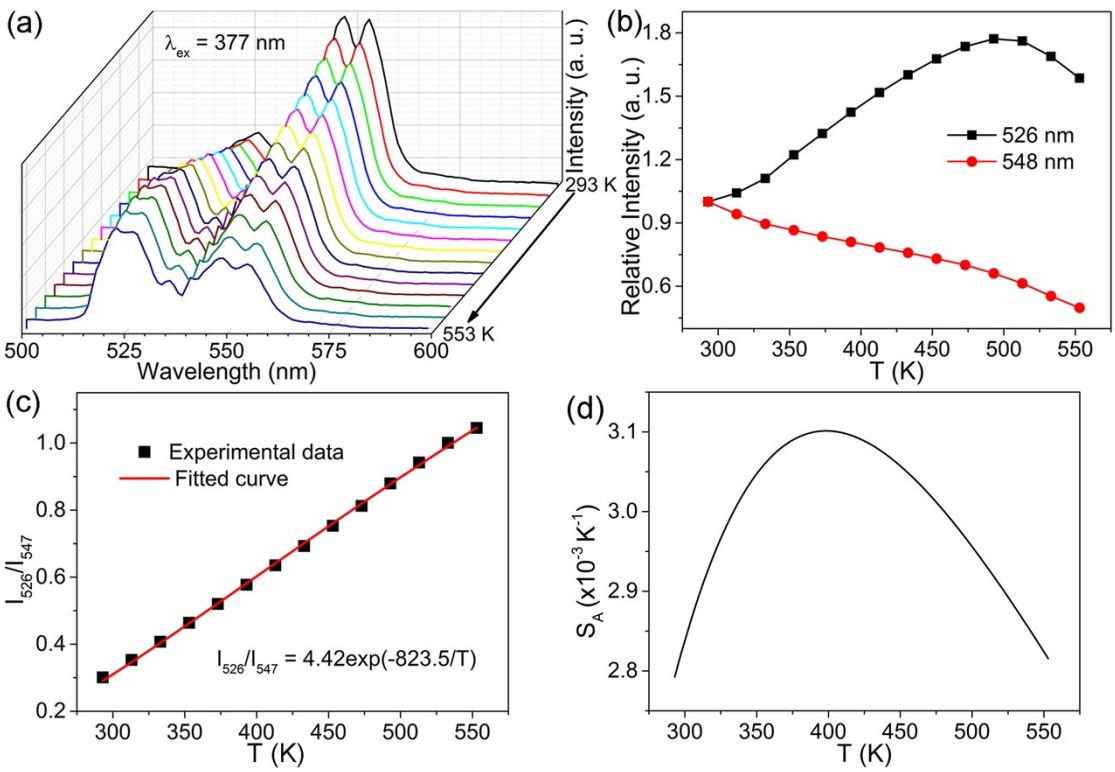

Fig. S4 (a) Emission spectra of GSO:10%Yb^{3+},1%Er^{3+} excited at 377 nm under various temperatures; (b) relative intensities of 526 and 548 nm emissions of Er^{3+} as a function of temperature; dependences of I_{526}/I_{548} on absolute temperature; (d) absolute and relative sensitivities of GSO:10%Yb^{3+},1%Er^{3+} as a function of absolute temperature

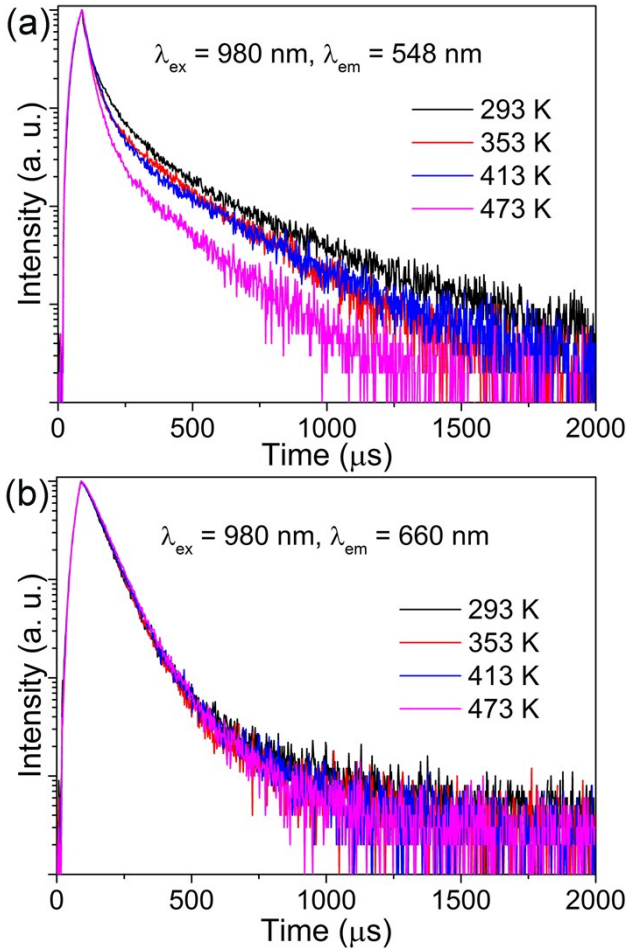

Fig. S5 Decay curves of GSO:10%Yb^{3+},0.25%Ho^{3+} under different temperatures by monitoring (a) 548 nm and (b) 660 nm

Table S1 τ_i and A_i values for GSO:10%Yb^{3+},0.25%Ho^{3+} by monitoring 548 nm under different temperatures

T (K)	τ_1 (μs)	τ_2 (μs)	A_1	A_2
298	40.2	252.6	6317.8	983.1
353	31.3	223.8	4986.1	855.5
413	34.4	247.2	7514.7	661.7
473	27.6	176.7	5709.7	492.7

Table S2 τ_i and A_i values for GSO:10%Yb^{3+},0.25%Ho^{3+} by monitoring 660 nm under different temperatures

T (K)	τ_1 (μs)	τ_2 (μs)	A_1	A_2
298	63.0	262.0	9411.3	199.5
353	64.2	248.3	9561.5	139.6
413	65.5	231.1	8789.2	203.0
473	67.9	204.6	9080.0	216.0